AD-A067 778 SOLAR TURBINES INTERNATIONAL SAN DIEGO CA F/G 11/2
STUDY OF EROSION MECHANISMS OF ENGINEERING CERAMICS.(U)
MAR 79 M E GULDEN N00014-73-C-0401
UNCLASSIFIED RDR-1778-9 NL

1 OF 1
AD
A067 778

END
DATE
FILMED
6-79
DDC

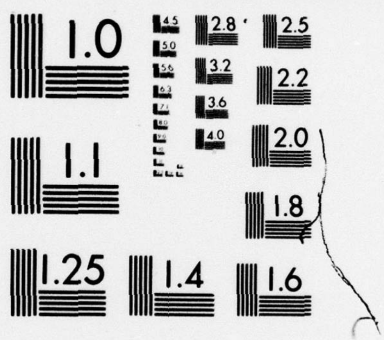


MICROCOPY RESOLUTION TEST CHART
NATIONAL BUREAU OF STANDARDS-1963-A

LEVEL III

March 1979

A045216

12

# Study of Erosion Mechanisms of Engineering Ceramics

Seventh Interim Technical Report

**Effect of Number of Impacts on Erosion in the Elastic-Plastic Response Regime**

AD A067778

Prepared Under Contract N00014-73-C-0401
NR0-32-542

by
M.E. Gulden

DDC FILE COPY

for

**OFFICE OF NAVAL RESEARCH**
**DEPARTMENT OF THE NAVY**





**SOLAR TURBINES INTERNATIONAL**
**An Operating Group of International Harvester**

79 04 16 016

11 March 1979

12 24p.

6

# Study of Erosion Mechanisms of Engineering Ceramics .

9 Seventh Interim Technical Report. no. 7,

**Effect of Number of Impacts on Erosion in the Elastic-Plastic Response Regime**

15 Prepared Under Contract N00014-73-C-0401
NR0-32-542

by


10 Mary Ellen M.E. Gulden


for

**OFFICE OF NAVAL RESEARCH**
**DEPARTMENT OF THE NAVY**





326 550


**SOLAR TURBINES INTERNATIONAL**
**An Operating Group of International Harvester**
2200 Pacific Highway, P.O. Box 80966, San Diego, California 92138




14 RDR-1778-9

SR79-R-4861-09
(RDR 1778-9)


79 04 16 016

## Table of Contents





[redacted]

## List of Figures



## List of Tables

## ABSTRACT

A $MgF_2$ target was subjected to impact conditions from single particle to $10^{10}$ impacts which simulated a natural dust environment (quartz particles) in the subsonic velocity regime. The function of particle size and velocity predicted by the "elastic-plastic" impact model is followed for this system. Impact damage is characterized by a heavily deformed contact area between particle and target, with radial cracks propagating outward from the contact zone, and with subsurface lateral cracks propagating outward on planes nearly parallel to the surface. The laterally cracked material is responsible for most of the erosion loss. This type of damage is also consistent with the "elastic-plastic" model. For a given particle size - velocity condition the volume of material removed for a single impact can vary over three orders of magnitude. This large variation is due primarily to differences in particle orientations during impact which results from the irregular angular natural quartz particles. For these conditions there is not a significant difference between the amount of material removed for the first impact and for subsequent impacts on the damage area of the initial impact. The results imply that there is not an incubation period or damage enhancement effect for erosion in the elastic-plastic impact response regime.

## I. INTRODUCTION

Solid particle erosion can be a severe life-limiting constraint. In recent years considerable interest has been shown in the use of ceramics for gas turbine engine components, bearings, valves, heat exchangers, and radome and infrared transparent windows. A knowledge of impact damage and erosion behavior is necessary before ceramics can be used with confidence in these systems.

Recent investigations have shown that a number of erosion mechanisms for ceramics can exist and that erosion and impact is a complex process (Refs. 1 2, 3 and 4). Essentially, two types of models have been proposed for solid particle impact (single particle) and erosion (multi particle) of brittle materials. The earlier models were based on elastic interaction between target and particle and predicted that material removal occurs by the intersection of ring cracks on the target surface. This process has been observed on several materials under static and low velocity impact conditions with relatively large spherical particles (Refs. 3 and 4). More recent analysis has treated static and dynamic plastic indentation, which is characterized by plastic deformation of the contact area between the particle and the target, with radial cracks propagating outward from the contact zone, and with subsurface lateral cracks propagating outward on planes nearly parallel to the surface. This type of damage, termed "elastic-plastic", is observed for impact with angular particles of generally greater compressibility than the target (Refs. 1 and 2). The model predicts that

$$\text{Erosion} \propto V^{3.2} R_p^{3.7} \rho_p^{0.25} / K_c^{1.3} H^{0.25}$$

where V is particle velocity, $R_p$ is particle radius, $\rho_p$ is particle density, and $K_c$ and H are target fracture toughness and hardness, respectively.

These models are based on single impacts and were developed for isotropic materials under idealized conditions. Significant erosion of structural components generally requires multi particle impacts. The usefulness of the models for explaining and predicting actual erosion behavior is dependent in part on the effect of number of impacts on material loss. It is known that for rain erosion and for solid particle erosion occurring by intersecting ring cracks (elastic interaction) that an incubation period exists prior to the onset of uniform erosion (Refs. 3 and 5). That is, material loss per impact is minor for initial or single impacts compared with material loss per impact after uniform erosion has initiated. The effect of number of impacts on erosion loss under conditions of "elastic-plastic" indentation has not been investigated previously. For this type of damage process the major source of material removal is the laterally cracked material (Refs. 1 and 2).

The results of an investigation to determine the effect of number of impacts on erosion in the elastic-plastic impact response regime are presented. The experimental approach was to perform tests in a controlled manner to simulate a service dust environment in the subsonic velocity regime.

## II. EXPERIMENTAL PROCEDURE

### 2.1 MATERIALS

The target material used for this investigation is Irtran 1, hot-pressed $MgF_2$, a common infrared window material. Unless otherwise noted, the starting surface was in the polished condition. Angular, high purity quartz was used for the impacting particles. Quartz was chosen because in previous work on metals, it was found to be the principal erosive component in natural dust, i.e., the amount of erosion was directly proportional to the percentage of quartz in the natural dusts (Ref. 6). Six particle size ranges were used as follows: less than 30, 44-53, 53-74, 105-125, 250-297 and 350-420 µm. These size ranges were chosen to be representative of airborne dust and to provide significant particle mass differences of at least one half order of magnitude. Properties of the target and particles considered pertinent to erosion response are listed in Table 1.

This target-particle system was selected because previous work has shown that impact and erosion occurs by the elastic-plastic impact type of damage process (Ref. 2).

Table 1
Physical Properties of Target and Particles

| | Elastic Modulus (GPa) | Fracture Toughness (MPa $m^{1/2}$) | Hardness* (GPa) | Acoustic Impedance ($Kgm^{-2}s^{-1}$ x $10^7$) | Structure |
|---|---|---|---|---|---|
| Hot pressed $MgF_2$ (Irtran) | 117 | 1.0 | 6 | 3.2 | Single phase ∿2μ grain size |
| Natural quartz | 95 | ∿0.7 | ∿6 | 1.6 | |

* The hardnesses are the quasi-static Vickers hardness in the macro indentation load independent regime.

## 2.2 EROSION TESTING

Erosion tests were performed with a stationary target impacted by particles accelerated in an air stream. Particles are injected into the stream three meters from the target to provide sufficient distance for acceleration. The air velocity variations across the 0.95 cm diameter nozzle is less than five percent and velocity is varied between 15 and 343 m/sec to achieve the desired particle velocity. Particle velocity is measured using the rotating double disc technique described in Reference 7. Five velocities for each particle size range were used to establish erosion rates. The particles are fed into the gas stream using a precision feeder at a sufficiently low concentration that particle interactions in the carrier gas stream or on the target surface are negligible. A detailed description of the erosion test apparatus is given in Reference 6.

All erosion tests were performed at 90-degree impingement angles at ambient temperatures. Perpendicular impingement is at or near that for maximum erosion of brittle materials. The number of particles per test was varied from a few particles (to examine single particle impacts) to as many as $10^{10}$ particles (to insure uniform erosion) over a 0.71 $cm^2$ target area. For the long time - large number of particle tests, the specimens were weighed at specific intervals to assess any changes in erosion with number of impacts.

Three series of tests were performed to assess the effect of number of impacts on erosion of $MgF_2$ impacted with quartz particles. These can be conveniently separated into the following: weight loss changes as a function of number of impacting particles, effect of starting surface finish on erosion weight loss, and examination and measurement of single and second impacts on the damage area of the initial impact.

## III. EXPERIMENTAL RESULTS AND DISCUSSION

### 3.1 WEIGHT LOSS DUE TO EROSION

For the system $MgF_2$ target-quartz particles eroded under the conditions given above (five particle size ranges, five velocities) and for conditions of heavy erosion, it was found that volume loss per particle did follow the function of particle size and velocity predicted by the elastic-plastic impact model. The results are shown in Figure 1. The relationship is valid over the entire range of particle size and velocity, indicating that the same erosion mechanism is operative for these conditions.

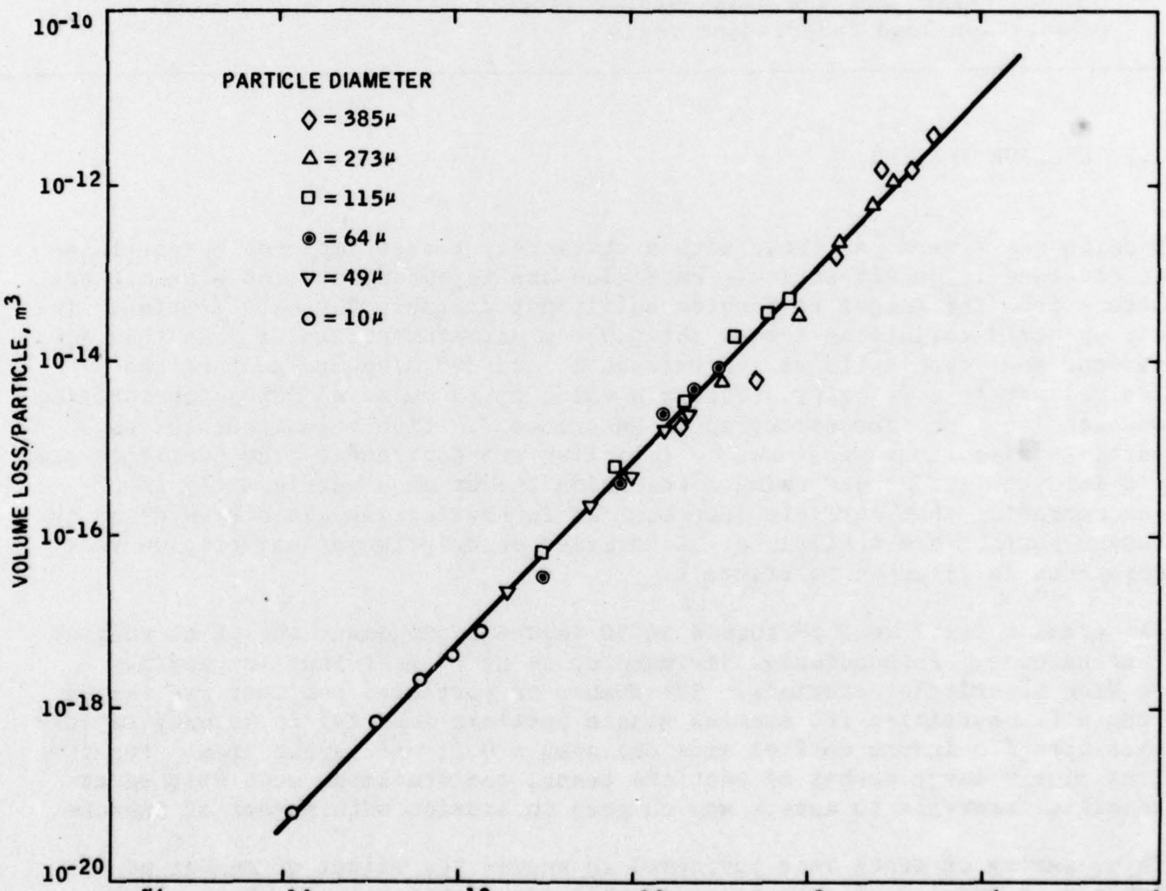


Figure 1. Erosion Versus the Function of Particle Size and Velocity Predicted by Elastic-Plastic Model for $MgF_2$ Impacted With Quartz Particles (Velocity Varied Between 40 and 285 m/sec)

The effect of a progressive number of impacts on erosion loss per impact is shown in Figure 2. The data is normalized by $R^{3.7}V^{3.2}$ to allow comparison of all particle sizes and velocities. There is no consistent effect of number of impacts on the erosion loss per particle at least between $10^3$ and $10^{10}$ particles and the majority of data points fall in a one order of magnitude band. It is considered that the slight increase in volume loss for impact with $10^2$ particles is also not significant because weight losses are less than a milligram and experimental error is maximized for these conditions. For a given test condition, experimental error is confined to ~0.25 order of magnitude.

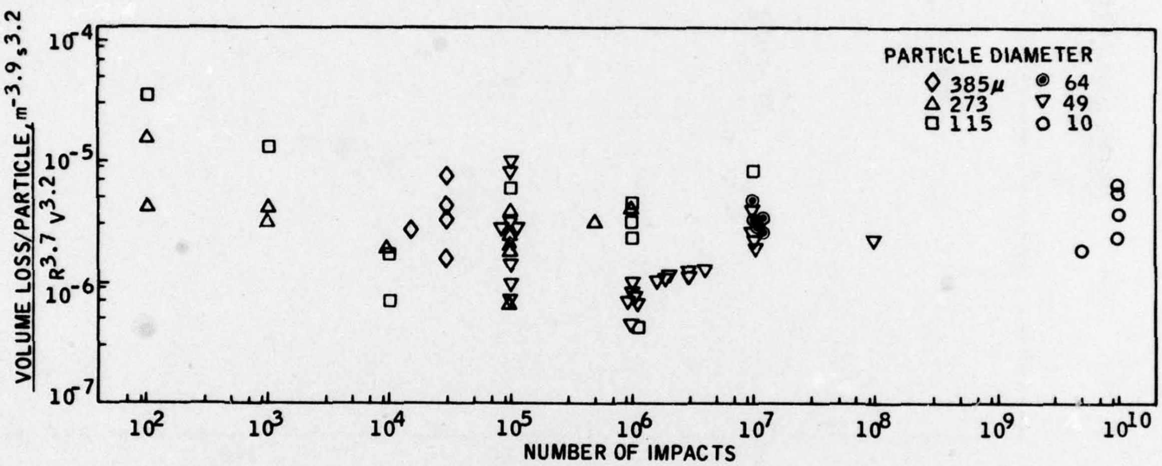


Figure 2. Erosion Weight Loss Normalized by $R^{3.7}V^{3.2}$ Versus Total Number of Impacting Particles

The data as shown in Figure 2 does not account for the number of particles which have impacted on a previously impacted area of the target. A statistical estimate of the number of impacts required to totally damage the target one layer deep can be made by dividing the total target area subjected to erosion by the area damaged per impact. The damaged area was measured for single impacts. This area varies appreciably with particle size and velocity, and thus the number of impacts to cover also varies. In Figure 3, the erosion weight loss data, again normalized by $R^{3.7}V^{3.2}$, is plotted versus the number of impacts on a single impact area. Appreciable scatter is evident, particularly for the initial impacts and there is no statistically significant effect of multiple impacts on the amount of material removed per impact. In other words, the amount of material removed on the first impact is not significantly different from that removed by the 50th impact on the same area. These results suggest that for this system, there is no incubation period prior to onset of uniform erosion, nor is there removal enhancement caused by the residual cracks and flaws produced during initial impacts.

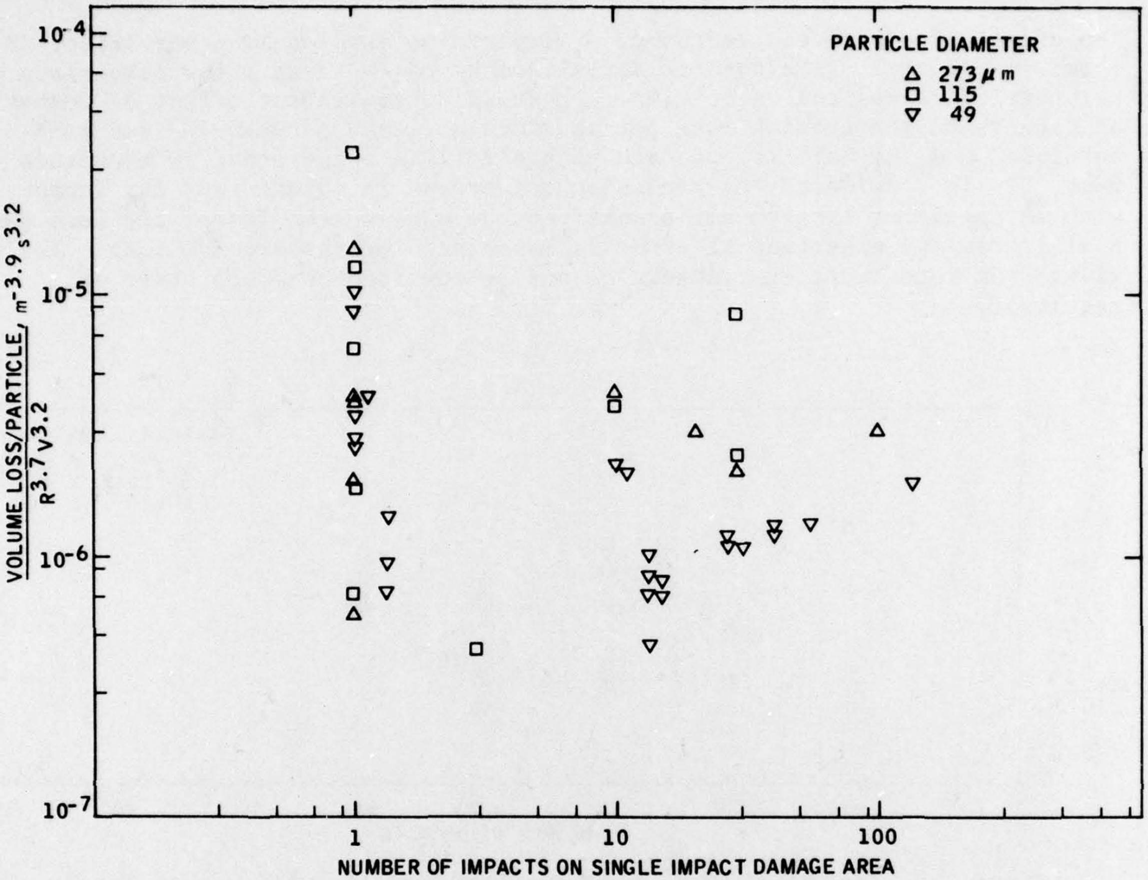


Figure 3. Erosion Weight Loss Normalized by $R^{3.7}V^{3.2}$ Versus Number of Impacts on Single Impact Damage Area

To elucidate the effect of starting surface finish on erosion loss, a series of tests were performed using 49 μm particles impacting on surfaces previously eroded with 273 μm particles, and the results were compared with polished starting surfaces. For a given velocity, the cracks and flaws produced by 273 μm particles are an order of magnitude larger than those produced by 49 μm particles. Two 273 μm pre-erosion surfaces were tested. One had been eroded with $10^3$ particles which statistically does not quite cover the surface with damage. This condition corresponds to a damage depth including radial cracks of ∿25 μm. The second condition was a heavily eroded surface ($10^5$ impacts) which corresponds to an erosion depth of ∿0.13 cm.

The results are shown in Figure 4. Weight loss is plotted versus weight of dust or number of impacts. Initially, more material is lost from the predamaged surfaces. However, the effect of this larger initial weight loss is not maintained since comparatively less material is removed from the predamaged surfaces than from the 49 μm eroded surfaces for the later tests. An explanation for this phenomenon is not apparent and further extensive experimental work would be necessary to elucidate this behavior. However,

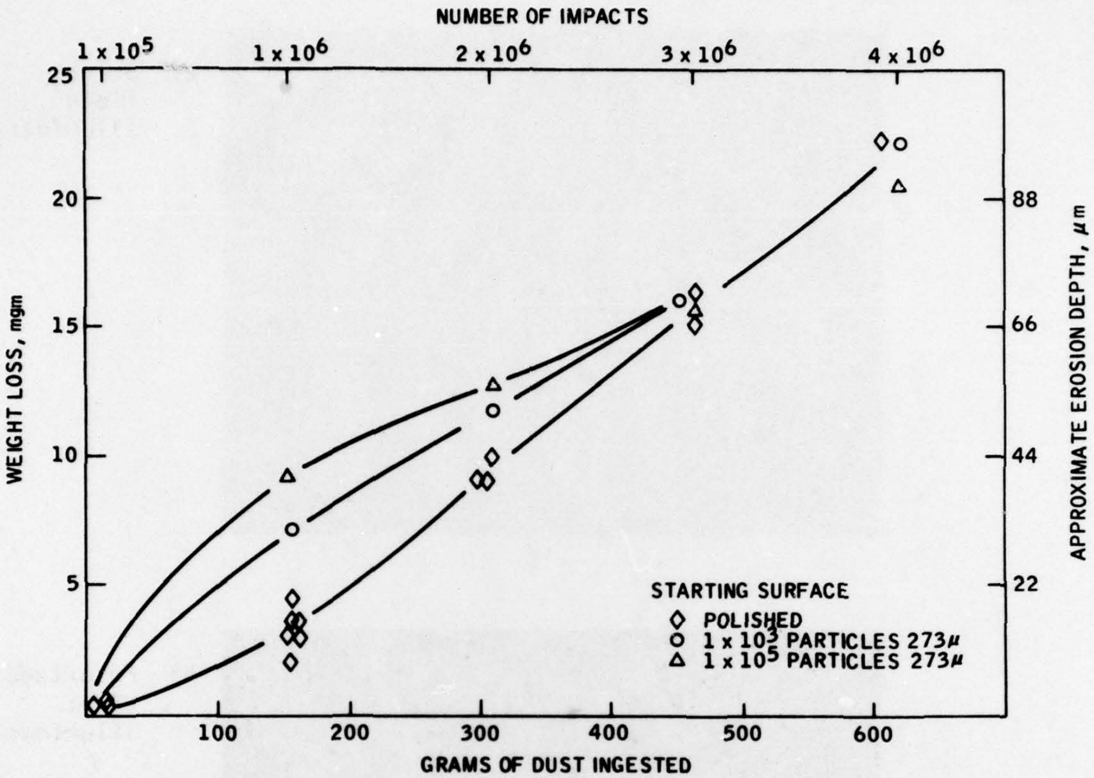


Figure 4. Effect of Starting Surface Finish on Erosion (49 μm, 247 mps Velocity)

these results indicate that starting surface finish is not a significant variable for conditions of heavy erosion. That is, any initial increase in weight loss due to a severely flawed starting surface is not maintained in later stages of erosion.

## 3.2 EXAMINATION OF IMPACTED AND ERODED SURFACES

The discussion to this point has dealt with erosion weight losses and as such has averaged the effects of many impacts. Surfaces were examined for a range of erosion conditions varying between single particle impacts and erosion to a depth of several grain diameters. Generally, the heavily eroded surfaces were sufficiently damaged that little information was provided concerning erosion mechanisms or processes. Since the impact and erosion models are based on the damage produced during a single particle impact, an examination of initial and subsequent impacts on the initially damaged area will provide information on the actual material removal process. A typical example of single impact damage is shown in Figure 5. Figure 5a was taken in bright field illumination and Figure 5b was taken in polarized light to reveal

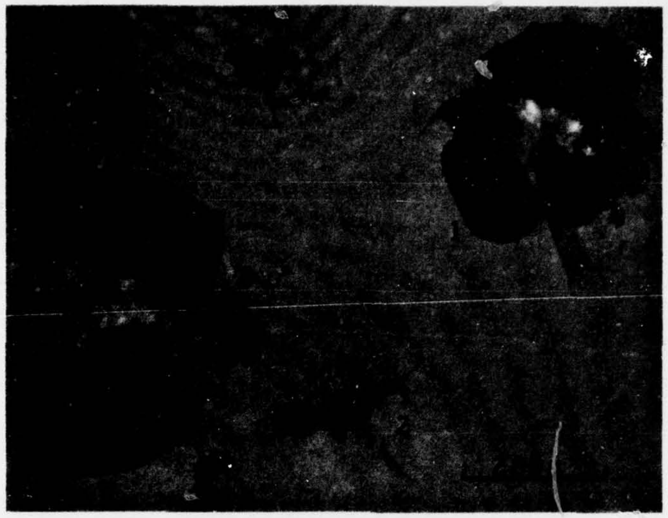

a) Bright Field Illumination

b) Polarized Light Illumination

Figure 5. Single Particle Impact Damage on $MgF_2$ Target Produced by 273 μm Quartz Particles Traveling at 190 mps

subsurface cracks. The damage is characterized by a central, highly deformed crater, with associated radial and lateral crack formation. The radial cracks extend outward from the particle contact zone and are generally perpendicular to the surface. Lateral cracks also extend from the contact zone but are subsurface and approximately parallel to the surface. This type of damage has been observed in several systems (Refs. 1, 2, 8) and is referred to as elastic-plastic impact. This type of damage was characteristic of the entire range of particle sizes and velocities investigated. Generally, the laterally cracked regions are responsible for the majority of material removal.

Figure 5 also illustrates the wide variation in single impact damage and removal for a given particle size-velocity combination. This is thought to be more a function of orientation of the impacting particle than of the target properties. The hot-pressed $MgF_2$ target is a single phase material with a 2 micron grain size and the surface was polished prior to impact. Any surface flaws or grain size and orientation effects are expected to be minimal compared with the size of the particle contact area and subsequent cracking. However, the particles can impact in a variety of orientations ranging from a corner oriented impact to a face oriented impact. Although particle mass and velocity for the two orientations is nominally the same, the energy transferred per unit area will vary appreciably. Additionally, the 273 μm average particle size encompasses a range between 250 to 297 μm which provides a mass variation.

Not only is there appreciable variation in single impact damage area, but there is more variation in the amount of material removed. In Figure 5a, a single layer of laterally cracked material has been removed from impacts 1 and 3, although additional laterally cracked material still exists (Fig. 5b). The amount of material removed from impacts 2 and 4 is comparatively insignificant, and the laterally cracked material (seen in Fig. 5b) has remained intact.

The effect of second impacts on prior impacted areas was investigated for three particle size-velocity conditions as follows: 273 μm - 190 mps, 273 μm - 120 mps and 115 μm - 220 mps. The area damaged, area removed, average depth of damage, number and size of radial and lateral cracks were documented for between 20 and 25 initial impacts for each condition. The same measurements, plus any additional material removal or crack extension from initial impacts, were made for second impacts which occurred on the damaged initial impact area. The number of second impacts documented ranged from 5 to 18 for each condition. An example of a second impact is shown in Figure 6 where a particle has impacted over a laterally cracked region on impact 1, Figure 5. In this particular example the second impact has loosened the laterally cracked material on which it impacted, but no additional material has been removed. The greater intensity of polarized light reflection indicates a wide crack (compare Figs. 5b and 6b). Also, there is no apparent effect of the initial impact on damage produced by the second impact. The type of damage, magnitude of damage and material removal of the second impact is almost identical with that of impact 4, Figure 5.

a) Bright Field Illumination

b) Polarized Light Illumination

Figure 6. Second Impact on Damaged Area of Impact 1, Figure 5 (273 μm - 190 mps)

For a given particle size-velocity impact condition, the measured volume of material removed varied over a three order of magnitude range. The normalized frequency distribution for area damaged, area removed and volume removed (area removed times depth of impact) is shown in Figure 7. As can be seen, there is more variation within a given particle size-velocity condition than between the three impact conditions. The large variation precludes determination of significant differences between initial and second impacts using standard statistical procedures. A comparison between arithmetic means and standard deviations calculated from common logarithms of the volume removed

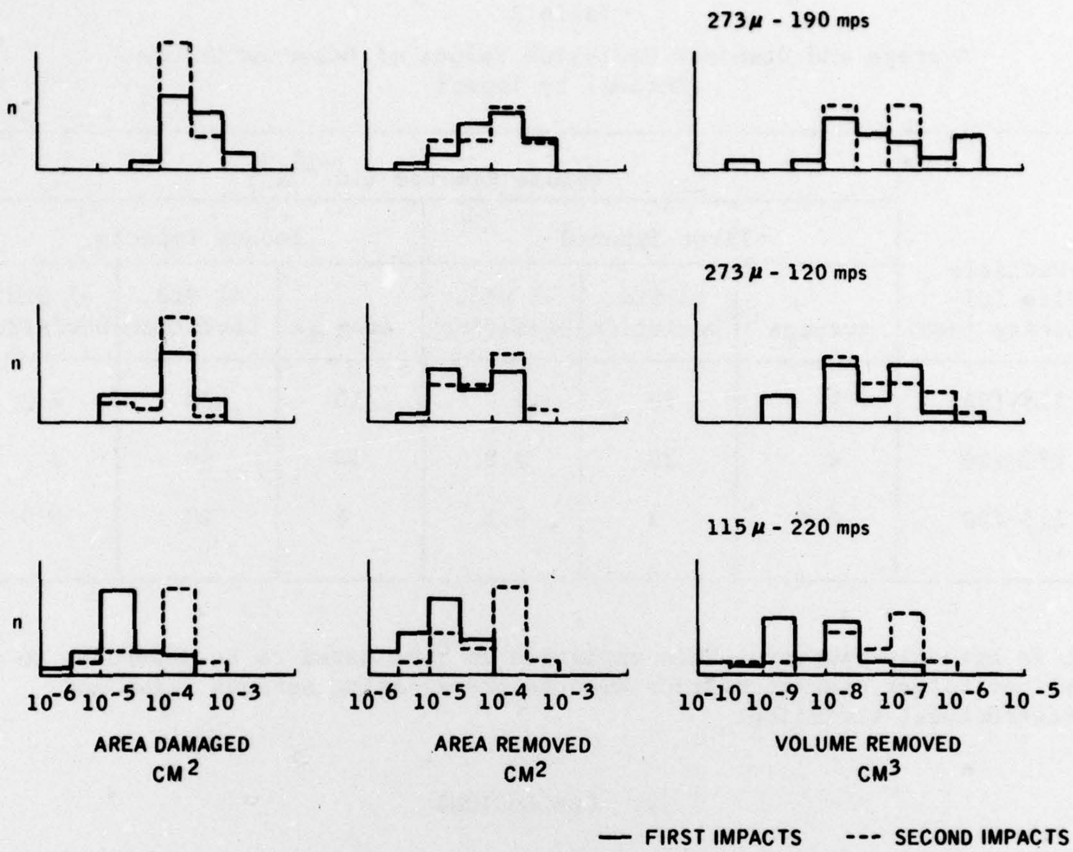


Figure 7. Frequency Distribution for Measured Impact Damage

indicate there is not a significant difference between the amount of material removed by the first impact and that removed by subsequent impacts on the initial impact damage area. These calculations are shown in Table 2. For impacts with 273 µm particles at both velocities, the average values for volume loss by second impacts are within the one standard deviation range for volume loss by the initial impacts. For impact with 115 µm particles, there is a one order of magnitude difference in average volume removed between the first and second impacts, but the one standard deviation ranges overlap.

For these test conditions, which simulate an airborne dust environment, there does not appear to be a significant difference between the amount of material removed by a single impact and that removed by a second impact on the damage area of the initial impact for a given particle size velocity condition.

To further elucidate the difference, if any, between first and second impacts, the data scatter will have to be reduced. A partial reduction could be accomplished by using spherical particles of a given size instead of the angular particles which encompassed a size range. However, some scatter would still be expected due to the variation in amount of cracked material

Table 2

Average and Standard Deviation Values of Measured Volume Removal by Impact

| Particle Size (μ)-Velocity (mps) | Volume Removed ($10^{-14} m^3$) | | | | | |
|---|---|---|---|---|---|---|
| | First Impacts | | | Second Impacts | | |
| | Average | +1 Std. Deviation | -1 Std. Deviation | Average | +1 Std. Deviation | -1 Std. Deviation |
| 273-190 | 9 | 70 | 1 | 10 | 70 | 2 |
| 273-120 | 4 | 20 | 0.8 | 10 | 50 | 2 |
| 115-220 | 0.6 | 3 | 0.1 | 6 | 40 | 0.9 |

that is actually removed. This variation is considered to be dependent on localized target characteristics such as pre-existing surface flaws and microstructural variation.

## IV. CONCLUSIONS

The results of this investigation indicate there is not a significant incubation or damage enhancement effect for conditions which simulate a dust erosion environment in the subsonic velocity regime when the damage is characterized by "elastic-plastic" impact. Any minor effect would be masked by the large (3 orders of magnitude) spread in volume removed per impact. This spread results primarily from variation in particle orientation during impact resulting from the angular quartz particles. The results further indicate that the model developed for "elastic-plastic" impact, which was based on single impacts, is applicable to heavy erosion conditions.

## V. ACKNOWLEDGEMENTS

This work was performed on Contract N00014-73-C-0401, sponsored by the Office of Naval Research, Department of the United States Navy. The writer appreciates the experimental assistance of R.B. Domes.

## VI. REFERENCES


1. Evans, A.G., Gulden, M.E. and Rosenblatt, M., Proc. Roy. Soc., Lond. A. 361 (1978), 343.

2. Gulden, M.E., "Solid Particle Erosion of High Technology Ceramics", to be published in A.S.T.M. STP Erosion: Prevention and Useful Applications.

3. Adler, W.F. and Sha, G.T., "Analytical Modeling of Subsonic Particle Erosion", Report AFML-TR-72-144, Wright-Patterson Air Force Base, Ohio (1972)

4. Oh, H.L., Oh, K.O.L., Vaidyanathan, S. and Finnie, I., "On the Shaping of Brittle Solids by Erosion and Ultrasonic Cutting", NBS Special Publication 348 (1972) 119.

5. Adler, W.F. and Hooker, S.V., "Characteristization of Transparent Materials for Erosion Resistance", Report No. AFML-TR-76-16, Wright-Patterson Air Force Base, Ohio (1976)

6. Smeltzer, C.E., Gulden, M.E., McElmury, S.S. and Compton, W.A., "Mechanisms of Sand and Dust Erosion in Gas Turbine Engines", USAAVLABS Tech. Report 70-36, Fort Eustis, VA (1970).

7. Ruff, A.W. and Ives, L.R., Wear, 35 (1975) 195.

8. Hockey, B.J., Widerhorn, S.M. and Johnson, H., "Erosion of Brittle Materials by Solid Particle Impact", in Fracture Mechanics of Ceramics Vol. 3, R.C. Bradt, D.P.H. Hasselman and F.F. Lange, Ed. Plenum Press (1978) 379.

<u>BASIC DISTRIBUTION LIST</u>

Technical and Summary Reports

Defense Documentation Center
Cameron Station
Alexandria, VA 22314 (12)

Office of Naval Research
Department of the Navy
Attn: Code 471 (1)
Code 102 (1)
Code 470 (1)

Commanding Officer
Office of Naval Research
Branch Office
495 Summer Street
Boston, MA 02210 (1)

Commanding Officer
Office of Naval Research
Branch Office
536 S. Clark Street
Chicago, IL 60605 (1)

Office of Naval Research
San Francisco Area Office
760 Market Street, Room 447
San Francisco, CA 94102
Attn: Dr. P. A. Miller (1)

Naval Research Laboratory
Washington, DC 20390
Attn: Code 6000 (1)
Code 6100 (1)
Code 6300 (1)
Code 6400 (1)
Code 2627 (1)

Naval Air Development Center
Code 302
Warminster, PA 18974
Attn: Mr. F.S. Williams (1)

Naval Air Propulsion Test Center
Trenton, NJ 08628
Attn: Library (1)

Naval Construction Batallion
Civil Engineering Laboratory
Port Hueneme, CA 93043
Attn: Materials Division (1)

Naval Electronics Laboratory Center
San Diego, CA 92152
Attn: Electron Materials
Sciences Division (1)

Naval Missile Center
Materials Consultant
Code 3312-1
Point Mugu, CA 93041 (1)

Commanding Officer
Naval Surface Weapons Center
White Oak Laboratory
Silver Springs, MD 20910
Attn: Library (1)

David W. Taylor Naval Ship R&D Center
Materials Department
Annapolis, MD 21402 (1)

Naval Undersea Center
San Diego, CA 92132
Attn: Library (1)

Naval Underwater System Center
Newport, RI 02840
Attn: Library (1)

Naval Weapons Center
China Lake, CA 93555
Attn: Library (1)

Naval Postgraduate School
Monterey, CA 93940
Attn: Mechanical Engineering Dept. (1)

Naval Air Systems Command
Washington, DC 20360
Attn: Code 52031 (1)
Code 52032 (1)
Code 329 (1)

Naval Sea System Command
Washington, DC 20362
Attn: Code 035 (1)

Naval Facilities
Engineering Command
Alexandria, VA 22331
Attn: Code 03 (1)

Scientific Advisor
Commandant of the Marine Corps
Washington, DC 20380
Attn: Code AX (1)

Naval Ship Engineering Center
Department of the Navy
CTR BG #2
3700 East-West Highway
Prince Georges Plaza
Hyattsville, MD 20782
Attn: Engineering Materials & Services Office, Code 6101 (1)

Army Research Office
Box CM, Duke Station
Durham, NC 27706
Attn: Metallurgy & Ceramics Division (1)

Army Materials & Mechanics Research Center
Watertown, MA 02172
Attn: Res. Programs Office (AMXMR-P) (1)

Air Force Office of Scientific Research
Bldg. 40
Bolling Air Force Base
Washington, DC 20332
Attn: Chemical Science Directorate (1)
Electronics & Solid State Sciences Directorate (1)

Air Force Materials Laboratory
Wright-Patterson Air Force Base
Dayton, OH 45433 (1)

Library
Building 50, Room 134
Lawrence Radiation Laboratory
Berkeley, CA 94710 (1)

NASA Headquarters
Washington, DC 20546
Attn: Code RRM (1)

NASA-Lewis Research Center
21000 Brookpark Road
Cleveland, OH 44135
Attn: Library (1)

National Bureau of Standards
Washington, DC 20234
Attn: Metallurgy Division (1)
Inorganic Materials Division (1)

Defense Metals and Ceramics Information Center
Battelle Memorial Institute
505 King Avenue
Columbus, OH 43201 (1)

Director
Ordnance Research Laboratory
P.O. Box 30
State College, PA 16801 (1)

Director, Applied Physics Laboratory
University of Washington
1013 Northeast 40th Street
Seattle, WA 98105 (1)

Metals and Ceramics Division
Oak Ridge National Laboratory
P.O. Box X
Oak Ridge, TN 37380 (1)

Los Alamos Scientific Laboratory
P.O. Box 1663
Los Alamos, NM 87544
Attn: Report Librarian (1)

Argonne National Laboratory
Metallurgy Division
P.O. Box 229
Lemont, IL 60439 (1)

Brookhaven National Laboratory
Technical Information Division
Upton, Long Island, NY 11973
Attn: Research Library (1)

## SUPPLEMENTARY DISTRIBUTION LIST

### Technical and Summary Reports

Dr. W. F. Adler
Effects Technology, Inc.
5383 Hollister Ave.
P.O. Box 30400
Santa Barbara, CA 92105

Dr. G. Bansal
Battelle Memorial Institute
505 King Avenue
Columbus, OH 43201

Dr. S. A. Bortz
IITRI
10 W. 35th Street
Chicago, IL 60616

Dr. J. D. Buch
Prototype Development Assoc., Inc.
1740 Garry Ave., Suite 201
Santa Ana, CA 92705

Dr. B. Budiansky
Harvard University
Dept. of Engineering and
Applied Science
Cambridge, MA 02138

Professor H. Conrad
University of Kentucky
Materials Department
Lexington, KY 40506

Dr. A. Cooper
Case Western Reserve University
Materials Department
Cleveland, OH 44106

Dr. N. Corney
Ministry of Defence
The Adelphi
John Adam Street
London, WC2N 6BB
United Kingdom

Dr. R. Bratton
Westinghouse Research Lab.
Pittsburgh, PA 15235

Dr. A. G. Evans
Rockwell International
P.O. Box 1085
1049 Camino Dos Rios
Thousand Oaks, CA 91360

Professor John Field
University of Cambridge
New Cavendish Laboratory
Cambridge, United Kingdom

Dr. I. Finney
University of California
Berkeley, CA 94720

Mr. A. F. Fyall
Royal Aircraft Establishment
Farnborough, Hants, United Kingdom

Dr. L. M. Gillin
Aeronautical Research Laboratory
P.O. Box 4331
Fisherman's Bend
Melbourne, VIC 3001, Australia

Ms. M. E. Gulden
Solar Turbines International
P.O. Box 80966
San Diego, CA 92138

Professor A. H. Heuer
Case Western Reserve University
University Circle
Cleveland, OH 44106

Dr. R. Hoaglund
Battelle Memorial Institute
505 King Avenue
Columbus, OH 43201

Dr. D. P. H. Hasselman
Montana Energy and MHD Research and
Development Institute
P. O. Box 3809
Butte, MT 59701

Mr. T. Derkus
TRW
Cleveland, OH 44117

Mr. E. Fisher
Ford Motor Company
Dearborn, MI 48121

Dr. P. Gielisse
University of Rhode Island
Kingston, RI 02881

Dr. S. Hart
Naval Research Laboratory
Washington, DC 20375

Professor G. Kino
Stanford University
Palo Alto, CA 94303

Professor R. Roy
Pennsylvania State University
Materials Research Laboratory
University Park, PA 16802

Dr. G. Schmidt
Air Force Materials Laboratory
Wright-Patterson Air Force Base
Dayton, OH 45433

Dr. R. A. Tanzilli
General Electric Company
Reentry & Environmental Systems Division
3198 Chestnut Street
Philadelphia, PA 19101

Dr. S. M. Wiederhorn
Inorganic Materials Division
National Bureau of Standards
Washington, DC 20234

Mr. J. Schuldies
AiResearch
Phoenix, AZ 85010

Dr. N. Tallan
Air Force Materials Laboratory
Wright-Patterson Air Force Base
Dayton, OH 45433

Mr. G. Hayes
Naval Weapons Center
China Lake, CA 93555

Dr. R. Jaffee
Electric Power Research Institute
Palo Alto, CA 94303

Dr. P. Jorgensen
Stanford Research Institute
Poulter Laboratory
Menlo Park, CA 94025

Dr. R. N. Katz
Army Materials & Mechanics Research Center
Watertown, MA 02171

Dr. H. Kirchner
Ceramic Finishing Company
P.O. Box 498
State College, PA 16801

Dr. L. Rubin
Aerospace Corporation
P.O. Box 92957
Los Angeles, CA 90009

Dr. D. A. Shockey
Stanford Research Institute
Poulter Laboratory
Menlo Park, CA 94025

Dr. T. Vasilos
AVCO Corporation
201 Lowell Street
Wilmington, MA 01887

Dr. R. Ruh
Air Force Materials Laboratory
Wright-Patterson Air Force Base
Dayton, OH 45433

Professor G. Sines
University of California, Los Angeles
Los Angeles, CA 90024

Mr. J. D. Walton
Engineering Experiment Station
Georgia Institute of Technology
Atlanta, GA 30332

Dr. B. R. Lawn
Physics Department
University of New South Wales
Kingston, New South Wales
Australia

Dr. Peter Heightman
Dept. 5827, W-5
Detroit Diesel Allison
Division of General Motors
P.O. Box 894
Indianapolis, IN 46206

UNCLASSIFIED

SECURITY CLASSIFICATION OF THIS PAGE (When Data Entered)

# REPORT DOCUMENTATION PAGE

READ INSTRUCTIONS BEFORE COMPLETING FORM

**1. REPORT NUMBER**

**2. GOVT ACCESSION NO.**

**3. RECIPIENT'S CATALOG NUMBER**

**4. TITLE (and Subtitle)**
Study of Erosion Mechanisms of Engineering Ceramics

**5. TYPE OF REPORT & PERIOD COVERED**
Seventh Interim Technical Report [illegible]

**6. PERFORMING ORG. REPORT NUMBER**
SR79-R-4061-09

**7. AUTHOR(s)**
Mary Ellen Gulden

**8. CONTRACT OR GRANT NUMBER(s)**
N00014-73-C-0401

**9. PERFORMING ORGANIZATION NAME AND ADDRESS**
Solar Turbines International
P.O. Box 80966
San Diego, California 92138

**10. PROGRAM ELEMENT, PROJECT, TASK AREA & WORK UNIT NUMBERS**
NR032-542

**11. CONTROLLING OFFICE NAME AND ADDRESS**
Department of the Navy
Office of Naval Research
Arlington, VA 22217

**12. REPORT DATE**
March 1979

**13. NUMBER OF PAGES**
15

**14. MONITORING AGENCY NAME & ADDRESS (if different from Controlling Office)**

**15. SECURITY CLASS. (of this report)**
UNCLASSIFIED

**15a. DECLASSIFICATION/DOWNGRADING SCHEDULE**

**16. DISTRIBUTION STATEMENT (of this Report)**
Distribution of this document is unlimited.

**17. DISTRIBUTION STATEMENT (of the abstract entered in Block 20, if different from Report)**

**18. SUPPLEMENTARY NOTES**
--

**19. KEY WORDS (Continue on reverse side if necessary and identify by block number)**
Solid Particle Erosion
Magnesium Fluoride
"Elastic-Plastic" Impact
Ceramics

the $10^{th}$ power

**20. ABSTRACT (Continue on reverse side if necessary and identify by block number)**
A $MgF_2$ target was subjected to impact conditions from single particle to $10^{10}$ impacts which simulated a natural dust environment (quartz particles) in the subsonic velocity regime. The function of particle size and velocity predicted by the "elastic-plastic" impact model is followed for this system. Impact damage is characterized by a heavily deformed contact area between particle and target, with radial cracks propagating outward from the contact zone, and with subsurface lateral cracks propagating outward on planes nearly parallel to the surface. The laterally cracked material is responsible for

DD FORM 1 JAN 73 1473 EDITION OF 1 NOV 65 IS OBSOLETE

UNCLASSIFIED

SECURITY CLASSIFICATION OF THIS PAGE (When Data Entered) most of the erosion loss. This type of damage is also consistent with the "elastic-plastic" model. For a given particle size - velocity condition the volume of material removed for a single impact can vary over three orders of magnitude. This large variation is due primarily to differences in particle orientations during impact which results from the irregular angular natural quartz particles. For these conditions there is not a significant difference between the amount of material removed for the first impact and for subsequent impacts on the damage area of the initial impact. The results imply that there is not an incubation period or damage enhancement effect for erosion in the "elastic-plastic" impact response regime.